

AIRS Subpixel Cloud Characterization Using MODIS Cloud Products

JUN LI

Cooperative Institute for Meteorological Satellite Studies, University of Wisconsin—Madison, Madison, Wisconsin

W. PAUL MENZEL

NOAA/NESDIS Office of Research and Applications, Madison, Wisconsin

FENGYING SUN

Cooperative Institute for Meteorological Satellite Studies, University of Wisconsin—Madison, Madison, Wisconsin

TIMOTHY J. SCHMIT

NOAA/NESDIS Office of Research and Applications, Madison, Wisconsin

JAMES GURKA

NOAA/NESDIS Office of System Development, Silver Spring, Maryland

(Manuscript received 28 May 2003, in final form 16 April 2004)

ABSTRACT

The Moderate Resolution Imaging Spectroradiometer (MODIS) and the Atmospheric Infrared Sounder (AIRS) measurements from the Earth Observing System's (EOS's) *Aqua* satellite enable improved global monitoring of the distribution of clouds. MODIS is able to provide, at high spatial resolution ($\sim 1\text{--}5$ km), a cloud mask, surface and cloud types, cloud phase, cloud-top pressure (CTP), effective cloud amount (ECA), cloud particle size (CPS), and cloud optical thickness (COT). AIRS is able to provide CTP, ECA, CPS, and COT at coarser spatial resolution (~ 13.5 km at nadir) but with much better accuracy using its high-spectral-resolution measurements. The combined MODIS–AIRS system offers the opportunity for improved cloud products over those possible from either system alone. The key steps for synergistic use of imager and sounder radiance measurements are 1) collocation in space and time and 2) imager cloud amount, type, and phase determination within the sounder pixel. The MODIS and AIRS measurements from the EOS *Aqua* satellite provide the opportunity to study the synergistic use of advanced imager and sounder measurements. As the first step, the MODIS classification procedure is applied to identify various surface and cloud types within an AIRS footprint. Cloud-layer information (lower, midlevel, or high clouds) and phase information (water, ice, or mixed-phase clouds) within the AIRS footprint are sorted and characterized using MODIS 1-km-spatial-resolution data. The combined MODIS and AIRS data for various scenes are analyzed to study the utility of the synergistic use of high-spatial-resolution imager products and high-spectral-resolution sounder radiance measurements. There is relevance to the optimal use of data from the Advanced Baseline Imager (ABI) and Hyperspectral Environmental Suite (HES) systems, which are to fly on the Geostationary Operational Environmental Satellite (GOES)-R.

1. Introduction

The Atmospheric Infrared Sounder (AIRS) instrument on board the Earth Observing System (EOS) *Aqua* satellite, the Hyperspectral Environmental Suite (HES) on the Geostationary Operational Environmental Satellite [(GOES)-R and beyond], the Cross-track Infrared Sounder (CrIS) of the National Polar-Orbiting Opera-

tional Environmental Satellite System (NPOESS), and the Infrared Atmospheric Sounding Interferometer (IASI) on the European Organization for the Exploitation of Meteorological Satellites (EUMETSAT) Meteorological Operational Weather Satellite (METOP) series will provide greatly enhanced remote sensing capabilities for observing the three-dimensional atmospheric temperature, moisture, and cloud structure. The significant new information on multilayer clouds retrieved from AIRS, HES, CrIS, and IASI will build upon the more limited cloud characterization that started with lower-spectral-resolution sounders such as the High

Corresponding author address: Dr. Jun Li, CIMSS/SSEC, University of Wisconsin—Madison, 1225 West Dayton Street, Madison, WI 53706.
E-mail: jun.li@ssec.wisc.edu

Resolution Infrared Sounder (HIRS) (Smith et al. 1979; Susskind et al. 1987) and GOES sounder (Menzel and Purdom 1994; Schmit et al. 2002; Menzel et al. 1992).

The Moderate Resolution Imaging Spectroradiometer (MODIS) on board the EOS *Terra* and *Aqua* satellites provides multispectral measurements with 1-km resolution. Cloud properties retrieved include the cloud mask (Ackerman et al. 1998), classification mask (Li et al. 2003), cloud phase (Strabala et al. 1994; Baum et al. 2000) with 1-km spatial resolution, cloud-top pressure (CTP), effective cloud amount (ECA; which is defined as the product of cloud emissivity and fractional cloud coverage) with 5-km spatial resolution (Frey et al. 1999; Zhang and Menzel 2002), cloud particle size (CPS), and cloud optical thickness (COT) at the visible band (King et al. 2003). The Advanced Baseline Imager (ABI; Schmit et al. 2002) on GOES-R and beyond will have instrumental capabilities comparable to MODIS but will also have high temporal resolution.

Cloud parameters such as CTP, ECA, CPS, and COT can be retrieved with better accuracy from AIRS cloudy radiance measurements used in combination with MODIS data within the AIRS footprint (Li et al. 2004). As the first fundamental step of the imager-sounder synergism, MODIS surface-type information (water, land, desert, snow, etc.), cloud-layer information (lower, mid-level, or high clouds), phase information (water, ice, or mixed-phase clouds) within each AIRS footprint are sorted and characterized. Subpixel cloud phase information from MODIS data is found to be very important for the CPS and COT retrievals from the AIRS radiance measurements. Cloud phase information is required for CPS and COT retrieval from IR radiance measurements.

Both MODIS and AIRS data for various scenes are analyzed to illustrate the utility of sounder subpixel cloud characterization. The technique for utilization of AIRS subpixel cloud characterization with MODIS imager data is also applicable to data from the operational ABI-HES system on GOES-R and beyond.

The purpose of this manuscript is to demonstrate how MODIS can improve AIRS subpixel cloud characterization and provide additional information for cloud parameter retrievals within a single AIRS footprint. It is important to note that use of MODIS data is not required for operational AIRS retrievals; the AIRS cloud-clearing processing (Susskind et al. 2003), using microwave data, is considered very robust. Use of MODIS-AIRS data for retrievals will benefit future imager and sounder systems (e.g., ABI-HES) specifically in the absence of microwave measurements. This study will be useful because (a) the collocated MODIS 1-km cloud phase mask indicates whether an AIRS subpixel contains water, ice, or mixed-phase clouds, which is required in the cloud microphysical property retrieval; and (b) the collocated MODIS 1-km classification mask helps to determine whether an AIRS subpixel is partly cloudy or overcast and whether it is characterized by single-layer or multilayer clouds.

Section 2 provides a summary of characteristics of AIRS and MODIS measurements. Section 3 describes the algorithms used for MODIS-AIRS collocation, MODIS surface- and cloud-type classification, and MODIS phase retrieval. Section 4 describes the results of AIRS subpixel cloud characterization and their application in retrieval of cloud properties. A discussion of issues affecting AIRS subpixel cloud characterization is given in section 5. Section 6 describes the conclusions and future work.

2. MODIS and AIRS on the *Aqua* platform

MODIS (information available online at <http://modis.gsfc.nasa.gov/>) is a key instrument on the EOS *Terra* and *Aqua* platforms for conducting global change research. MODIS provides global observations of Earth's land, oceans, and atmosphere in 36 bands. These include visible (VIS), near-infrared (NIR), and infrared (IR) regions of the spectrum from 0.4 to 14.5 μm every 1–2 days at horizontal resolutions ranging from 250 m to 1 km at nadir. Various types of MODIS atmospheric and cloud products (King et al. 2003; Platnick et al. 2003) have been available for the scientific community (detailed information about the MODIS products is available online at http://daac.gsfc.nasa.gov/CAMPAIGN_DOCS/MODIS/product_descriptions_modis.shtm1#mod04_12).

AIRS (Aumann et al. 2003; information online at <http://www-airs.jpl.nasa.gov>) is a high-spectral-resolution infrared sounder designed to obtain vertical profiles of atmospheric temperature and water vapor from the surface to an altitude of 40 km. AIRS has 2378 channels, measuring from 3.74 to 15.4 μm with a spectral resolving power $\lambda/\Delta\lambda = 1200$, where λ is the wavelength. AIRS provides IR information at a 13.5-km horizontal resolution at nadir. The AIRS products are described online (<http://aqua.nasa.gov/AIRS3.html>).

Figure 1 shows the AIRS brightness temperature (BT) image of channel 763 (901.69 cm^{-1}) at 1917 UTC (AIRS granule 193) 6 September 2002. The presence of cold clouds is indicated by the blue (cold) colors. The boxes (A1, A2, and A3) indicated in Fig. 1 are the areas studied in this paper.

3. Algorithms used in AIRS subpixel cloud characterization with MODIS data

a. Collocation between MODIS and AIRS measurements

MODIS pixels with 1-km spatial resolution are collocated within an AIRS footprint. Several collocation algorithms have been developed that are based on the scanning geometry of two instruments flown on the same satellite (Frey et al. 1996; Nagle 1998). With a set of AIRS earth-located observations, the footprint of each AIRS observation describes a figure that is circular

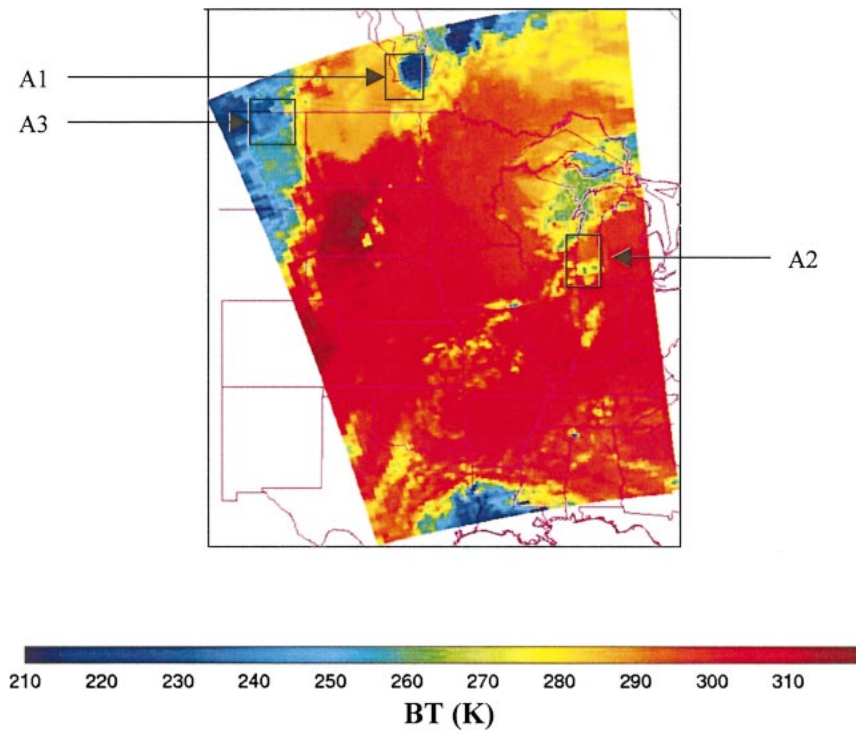


FIG. 1. The AIRS BT image of channel 763 (901.69 cm^{-1}) at 1917 UTC (AIRS granule number 193) 6 Sep 2002. The boxes (A1, A2, and A3) are the study areas in this paper.

at nadir, quasi ellipsoidal at intermediate scan angles, and ovalar at extreme scan angles. The diameter of the AIRS footprint at nadir is approximately 13.5 km. Assuming that the known satellite altitude is h kilometers, then the maximum value of the possible angular difference (θ_{\max} in radians) between the AIRS footprint and an overlapping earth-located MODIS observation at any scan angle is obtained by

$$\theta_{\max} = 57.295\,779\,5 \times 13.5/(2h). \quad (1)$$

The angular difference between the satellite-to-AIRS slant range (distance between the satellite and AIRS footprint on earth) and the satellite-to-MODIS slant range, falling within the limit θ_{\max} , is designated as overlapping the AIRS footprint. Depending on the angular difference between the AIRS and MODIS slant-range vectors, a weight is assigned to each MODIS pixel collocated to AIRS—1 if the MODIS pixel lies at the center of the AIRS oval, and 0 if it is at the outer edge. The collocation algorithm provides accuracy better than 1 km, provided that the geometry information from both instruments is accurate.

Figure 2 shows the study area A1 (see Fig. 1 for the location of the study area) of MODIS 11- μm BTs collocated to AIRS footprints. The circles in the figure are AIRS footprints with the shading of the footprints determined by the MODIS 1-km data. The warmer BTs represent midlevel and low clouds or the surface, while the cooler BTs represent high clouds. Most AIRS fields

of view (FOVs) appear homogeneous in terms of high-spatial-resolution MODIS observations, but some contain sub-AIRS FOV cloud features.

b. Summary of the MODIS surface- and cloud-type classification algorithm

Classification or clustering of the MODIS radiances is an important part of data analysis and image segmentation. A method for automated classification of surface and cloud types using MODIS radiance measurements has been developed (Li et al. 2003). The MODIS cloud mask information was used to define the training sets. Surface- and cloud-type classification is based on the maximum likelihood (ML) classification method (Haertel and Landgrebe 1999). Initial classification results define training sets for subsequent iterations. Iterations end when the number of pixels switching classes becomes smaller than a predetermined number or when other criteria are met. The mean vector in the spectral and spatial domain within a class is used for class identification, and a final 1-km-resolution classification mask is generated in a MODIS granule. Three parameter types (radiances, variances of radiances, and spectral BT differences) are used in the MODIS classification. All of the variables are determined at 1-km resolution. The MODIS classification mask assigns each MODIS pixel a surface (land, water, snow, desert, etc.) and cloud (lower, midlevels, high clouds, etc.) type.

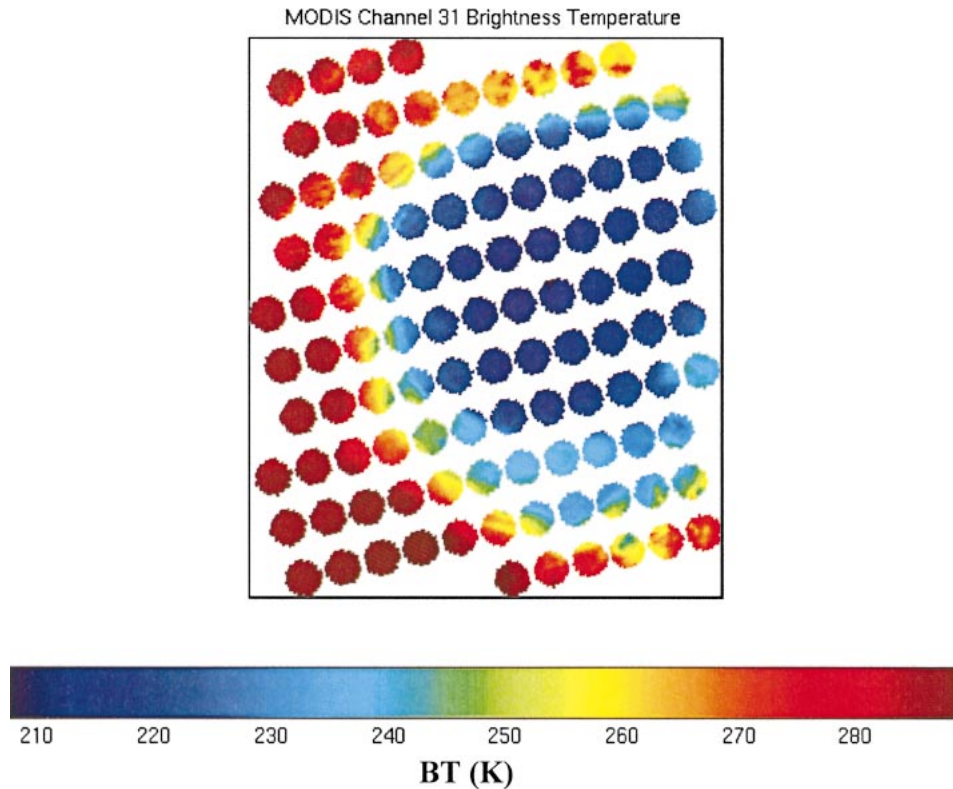


FIG. 2. The study area A1 (see Fig. 1 for the location of the study area) of MODIS 11- μm BTs collocated to AIRS footprints.

c. Summary of the MODIS cloud phase retrieval algorithm

The operational algorithm for MODIS cloud phase retrieval is used in this study. The basis for the inference of cloud phase from 8.5- to 11- μm MODIS bands is the difference of microphysical and optical properties between water droplets and ice crystals (Strabala et al. 1994; Baum et al. 2000). Radiative transfer simulations indicate that the BT difference between 8.5- and 11- μm bands (hereinafter denoted as $\text{BT}_{8.5-11}$) tends to be positive for ice clouds that have a visible optical thickness greater than approximately 1. Water clouds of relatively high optical thickness tend to exhibit negative $\text{BT}_{8.5-11}$ values of less than -2 K. The $\text{BT}_{8.5-11}$ value for lower clouds tends to become more negative as the water vapor loading increases and also as the surface emittance at 8.5- μm decreases. The $\text{BT}_{8.5-11}$ approach can be used for both daytime and nighttime retrievals. The IR phase algorithm is currently being run at 1-km resolution, and each MODIS cloudy pixel is flagged as having an uncertain phase, mixed phase, ice, or liquid water.

Figure 3 shows the MODIS cloud mask with the cloud phase (left panel) and classification mask (right panel) superimposed at 1-km resolution at 1920 UTC 6 September 2002. It shows that the pattern of water and ice clouds from the cloud phase mask is similar to the low

and high clouds, respectively, from the MODIS classification.

4. Application of AIRS subpixel cloud characterization using MODIS

Figure 4 shows the cloud phase retrievals (left panel) along with the classification results (right panel) at 1-km spatial resolution collocated to the AIRS footprints for the same study area A1 (see Figs. 1 and 2). The ice and water clouds within the AIRS footprints are well identified by the MODIS cloud phase mask. Some AIRS footprints contain mixed water and ice clouds. AIRS subpixel cloud phase characterization with the MODIS 1-km cloud phase mask is very important in retrieval of the cloud microphysical properties because a cloud-scattering model requires the cloud phase information. Single-layer high or low clouds within the AIRS footprints are well identified by the MODIS classification mask. Some AIRS footprints contain multilayer clouds (e.g., midlevel and low clouds). AIRS subpixel cloud classification with MODIS 1-km data provides useful information for AIRS profile retrieval and validation, as mentioned in section 1.

Figure 4 reveals that ice clouds in the MODIS cloud phase mask are highly correlated to the high clouds in

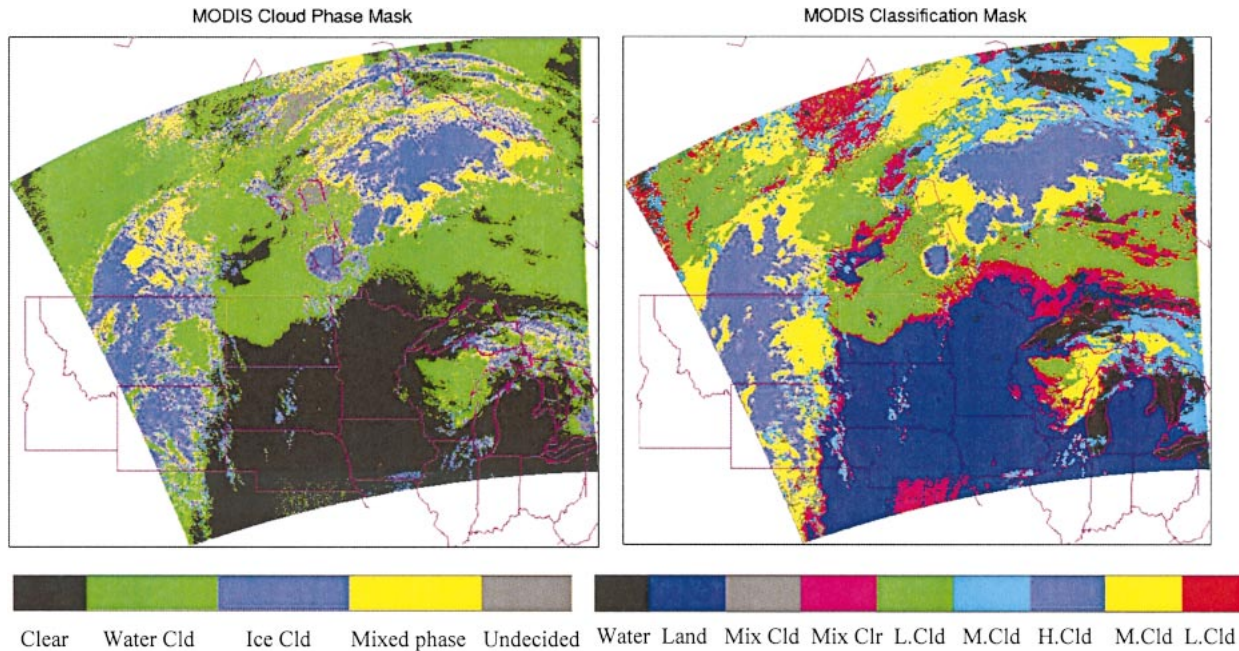


FIG. 3. The MODIS (left) cloud phase mask and (right) classification mask at 1-km spatial resolution at 1920 UTC 6 Sep 2002, covering part of AIRS granule 193 (see Fig. 1). L.Cld: low clouds, M.Cld: midlevel clouds, and H.Cld: high clouds.

the MODIS classification mask; similarly, water clouds are well related to the low clouds. Most clouds clearly identified as either ice or water phase in the MODIS cloud phase mask correspond to single-layer clouds in the MODIS classification mask. However, there are some AIRS footprints that have mixed cloud phases. Those clouds correspond to the multilayer clouds in the classification mask. The AIRS Science Team cloud parameter retrieval algorithm retrieves CTP and ECA for up to two cloud layers within each AMSU footprint (3×3 AIRS FOVs) using the assumption that the CTP

of each cloud layer is the same for the nine AIRS FOVs within the AMSU footprint (Susskind et al. 2003).

MODIS cloud phase mask information is useful in the microphysical cloud property retrieval using MODIS–AIRS data. Detailed algorithm and results on MODIS–AIRS synergistic retrieval will be discussed in a separate paper (Li et al. 2004). However, a brief description of the algorithm is given for a better understanding of the application of the AIRS subpixel cloud characterization.

The one-dimensional variational data assimilation

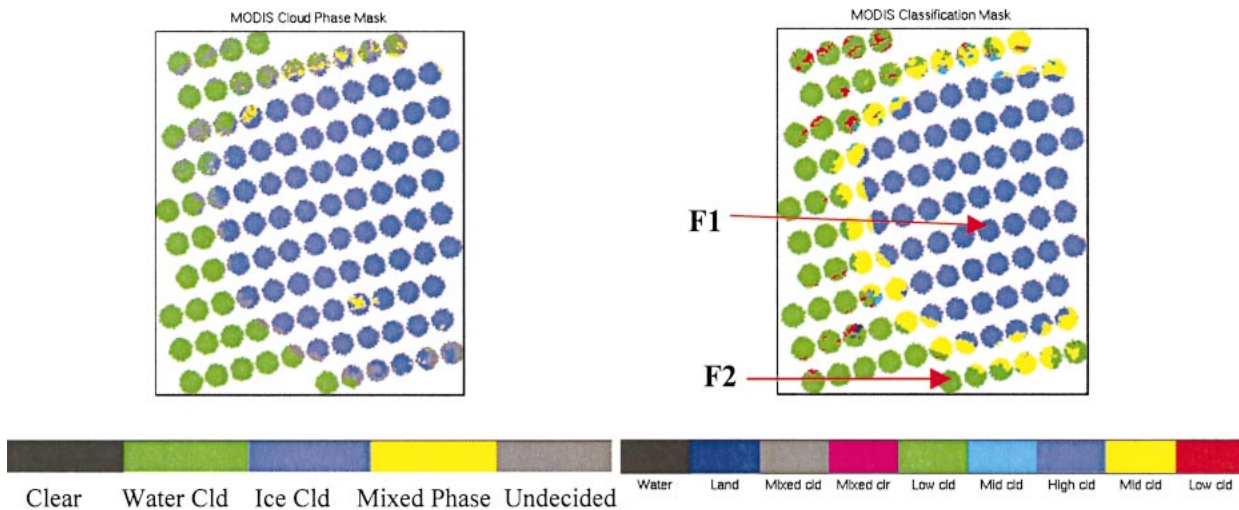


FIG. 4. The MODIS (left) cloud phase and (right) classification masks at 1-km spatial resolution for study area A1 (see Figs. 1 and 2) collocated to the AIRS footprints at 1920 UTC 6 Sep 2002.

(1DVAR) algorithm is used for the retrieval of cloud properties. Because 1DVAR requires background information that should be independent of AIRS measurements, the MODIS-derived CTP, ECA, CPS, and COT products are used as the background as well as the first-guess information to calculate the nonlinear optimal solution of cloud parameters from the AIRS longwave-spectral-band cloudy radiance measurements. Given the AIRS-observed cloudy radiance R for each channel, then the fast cloudy radiative transfer calculation $R = R(T, q, T_s, \epsilon_s, p_c, N\epsilon_c, D_c, OT_c)$ has the form

$$\mathbf{Y} = \mathbf{F}(\mathbf{X}), \quad (2)$$

where the vector \mathbf{X} contains the CTP (p_c), ECA ($N\epsilon_c$), CPS (D_c), and COT (OT_c) [the atmospheric temperature (T) profile, moisture (q) profile, surface skin temperature (T_s), and infrared surface emissivity (ϵ_s) are assumed to be known or are obtained from the forecast model analysis], and \mathbf{Y} contains N satellite-observed cloudy radiances. This fast cloudy forward model is derived from a coupled clear sky–fast radiative transfer model and a single-scattering fast cloud model. The stand-alone AIRS radiative transfer algorithm (SARTA) (Hannon et al. 1996; Strow et al. 2003; additional information online at <http://asl.umbc.edu/pub/rta/sarta/>) is used for AIRS clear-sky atmospheric transmittance calculation. Scattering and absorption effects of ice and water clouds are accounted for in a single scattering of the model that assumes ice clouds with hexagonal shapes for large particles and droxtals for small particles, and water clouds with spherical water droplets (Yang et al. 2001). The Lorenz–Mie theory is used to calculate the single-scattering properties. The cloud microphysical properties are described in terms of CPS and COT in the visible wavelength ($0.55 \mu\text{m}$). Given the visible COT and CPS, the IR COT, the single-scattering albedo, and the asymmetry factor can be parameterized for radiative effects of ice and water clouds. The cloudy radiance for a given AIRS channel can be calculated by combining the clear-sky optical thickness from SARTA and the COT, single-scattering albedo, and scattering phase function. Studies show that the slope of an IR cloudy BT spectrum between 790 ($12.6 \mu\text{m}$) and 960 ($10.4 \mu\text{m}$) cm^{-1} is sensitive to the CPS, while the cloudy radiances are sensitive to COT in the region of 1050 ($9.5 \mu\text{m}$)–1250 ($8 \mu\text{m}$) cm^{-1} for ice clouds (Yang et al. 2001).

The linear form of Eq. (2) is

$$\delta\mathbf{Y} = \mathbf{F}' \cdot \delta\mathbf{X}, \quad (3)$$

where \mathbf{F}' is the linear or tangent model of the fast cloudy forward model F . The 1DVAR approach is to minimize a penalty function $J(\mathbf{X})$, which measures how well the radiance measurements fit the background information, and possibly other physical constraints. A general form of the 1DVAR solution (Rodgers 1976; Eyre 1989) is given by

$$J(\mathbf{X}) = [\mathbf{Y}^m - \mathbf{Y}(\mathbf{X})]^T \mathbf{E}^{-1} [\mathbf{Y}^m - \mathbf{Y}(\mathbf{X})] + (\mathbf{X} - \mathbf{X}_B)^T \mathbf{B}^{-1} (\mathbf{X} - \mathbf{X}_B), \quad (4)$$

where the vector \mathbf{X} contains the CTP, ECA, CPS, and COT that need to be solved. Because ECA is spectrally dependent, ECAs at 10 wavenumbers (710, 720, 730, 740, 750, 760, 770, 780, 790, 800 cm^{-1}) are retrieved, and the ECA for a given channel will be obtained by linear interpolation from these 10 ECAs. Here, \mathbf{X}_B is the background information inferred from the MODIS operational products, \mathbf{Y}^m is the vector of the AIRS-measured cloudy radiances used in the retrieval process, $\mathbf{Y}(\mathbf{X})$ is a vector of cloudy radiances calculated from the cloud state \mathbf{X} , \mathbf{E} is the observation error covariance matrix that includes instrument noise plus the assumed forward model error, and \mathbf{B} is the assumed background error covariance matrix that constrains the solution. To solve Eq. (4), a Newtonian iteration is used,

$$\mathbf{X}_{n+1} = \mathbf{X}_n + J''(\mathbf{X}_n)^{-1} \cdot J'(\mathbf{X}_n), \quad (5)$$

and the following quasi-nonlinear iterative form (Eyre 1989) is obtained:

$$\delta\mathbf{X}_{n+1} = (\mathbf{F}_n'^T \cdot \mathbf{E}^{-1} \cdot \mathbf{F}_n' + \mathbf{B}^{-1})^{-1} \cdot \mathbf{F}_n'^T \cdot \mathbf{E}^{-1} \times (\delta\mathbf{Y}_n + \mathbf{F}_n' \cdot \delta\mathbf{X}_n), \quad (6)$$

where $\delta\mathbf{X}_n = \mathbf{X}_n - \mathbf{X}_B$ and $\delta\mathbf{Y}_n = \mathbf{Y}^m - \mathbf{Y}(\mathbf{X}_n)$. The AIRS channels with wavenumbers between 700 and 790 cm^{-1} are used for CTP and ECA retrieval while the IR longwave window channels with wavenumbers 790–950 and 1050–1130 cm^{-1} are used for the cloud microphysical property (CPS and COT) retrieval. The first guess \mathbf{X}_0 , or the starting point of the iteration in Eq. (6), is also the MODIS cloud products. The MODIS cloud products are well validated with the ground observations, such as lidar data; for example, Frey et al. (1999) compared MODIS Airborne Simulator (MAS) cloud retrievals with lidar observations and found that the CTP rms differences are within 50 hPa.

In order to compare cloud properties from MODIS–AIRS with those from AIRS alone, a minimum residual (MR) algorithm (Li et al. 2004) is used for the AIRS-alone cloud retrieval.

Different cloud cases are selected to demonstrate how the AIRS subpixel cloud characterization with MODIS data can help the MODIS–AIRS synergistic retrieval. From AIRS granule 193, containing 135 lines with each line containing 90 pixels, several AIRS footprints are selected as examples: 1) AIRS footprint F1 with thick, high-level clouds (line 125, pixel 44, see Fig. 4), 2) AIRS footprint F2 with thick, low-level clouds (line 121, pixel 41, see Fig. 4), 3) AIRS footprint F3 with partial cloudiness (line 70, pixel 80, see Fig. 7), and 4) AIRS footprint F4 with midlevel clouds (line 127, pixel 9, see Fig. 9) determined by the MODIS classification mask at 1-km spatial resolution. According to the MODIS cloud phase mask at 1-km spatial resolution collocated to AIRS footprints, F1 contains ice clouds while

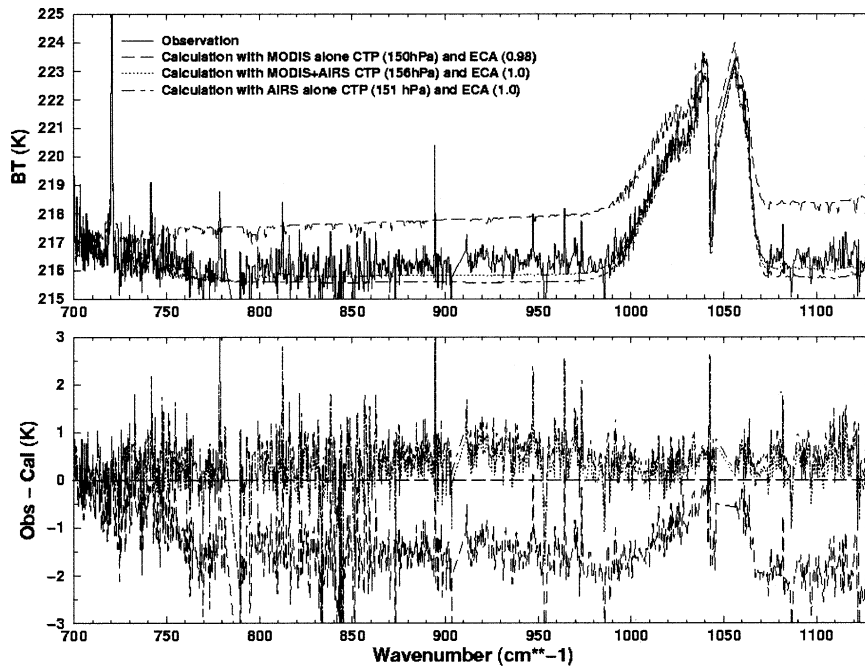


FIG. 5. (top) The AIRS longwave BT calculation from the MODIS-alone CTP and ECA (dashed line), the BT calculation from the AIRS-alone CTP and ECA (dot-dashed line), and the BT calculation from the MODIS-AIRS synergistically retrieved CTP and ECA (dotted line), as well as the BT observation (solid line) spectra for footprint F1 (see Fig. 4 for F1). (bottom) The corresponding BT difference between the observation and the calculation.

F2 contains water clouds. The upper panel of Fig. 5 shows the F1 cloudy BT calculation from the MODIS CTP and ECA (dashed line), the BT calculation from AIRS CTP and ECA (dot-dashed line), and the BT calculation from the MODIS-AIRS synergistically retrieved CTP and ECA (dotted line), as well as the cloudy BT observation (solid line). The lower panel of Fig. 5 shows the corresponding BT difference between the observation and the calculation. Both MODIS alone and AIRS alone did well for this high, thick cloud; AIRS alone is better than MODIS alone, and MODIS-AIRS is slightly better than AIRS alone. Figure 6 is the same as Fig. 5, but for footprint F2. Again, both MODIS alone and AIRS alone did well for this low, thick cloud, while MODIS-AIRS is better than either MODIS alone or AIRS alone. There is a better BT fit between the calculation and the observation with the MODIS-AIRS synergistically retrieved CTP and ECA than with that from either MODIS alone or AIRS alone. Also, the ECA retrievals from the MODIS-AIRS synergism, 1.0 for F1 (high clouds) and 0.88 for F2 (low clouds), are consistent with the MODIS classification mask collocated to these two AIRS footprints (MODIS classification mask indicates that both F1 and F2 are overcast).

Figure 7 shows the study area A2 (see Fig. 1 for the location of the study area). Footprint F3 views ice clouds in partly cloudy conditions based on the classification and cloud phase masks collocated to this footprint (not shown). Figure 8 shows that MODIS-AIRS produces

only a slight change in the MODIS-alone CTP; however, MODIS-AIRS changes the MODIS-alone ECA by 0.05 (only the IR 11- μm band is used in the MODIS ECA retrieval) and AIRS-alone ECA by 0.005. MODIS-AIRS changes the AIRS-alone CTP by 28 hPa. The ECA retrieval from the MODIS-AIRS synergism is 0.23, which is consistent with the MODIS 1-km classification mask collocated to F3 (see Fig. 7 for the classification mask). Although the calculation with MODIS-AIRS-retrieved CTP and ECA fits the observation very well in the CO_2 region (700–790 cm^{-1} , or 12.6–14.3 μm), there is still a discrepancy between the calculation and the observation in the IR window region (800–1130 cm^{-1} , or 8.8–12.5 μm) due to the scattering of ice clouds. Given retrieved CTP from MODIS-AIRS synergism, the CPS and COT can also be retrieved simultaneously from 800 (12.5 μm)–950 (10.5 μm) cm^{-1} and 1050 (9.5 μm)–1130 (8.8 μm) cm^{-1} with the variational approach. Again, the MODIS CPS and COT products serve as the background and first-guess information. Calculations that include the MODIS-AIRS estimates of CPS and COT fit well to the observations for all AIRS longwave channels (see also the solid line in Fig. 8).

Figure 9 shows the study area A3 (see Fig. 1 for the location of the study area) of the MODIS classification mask collocated to AIRS footprints. Footprint F4 represents midlevel ice clouds according to MODIS. Figure 10 shows that there is a large difference between the

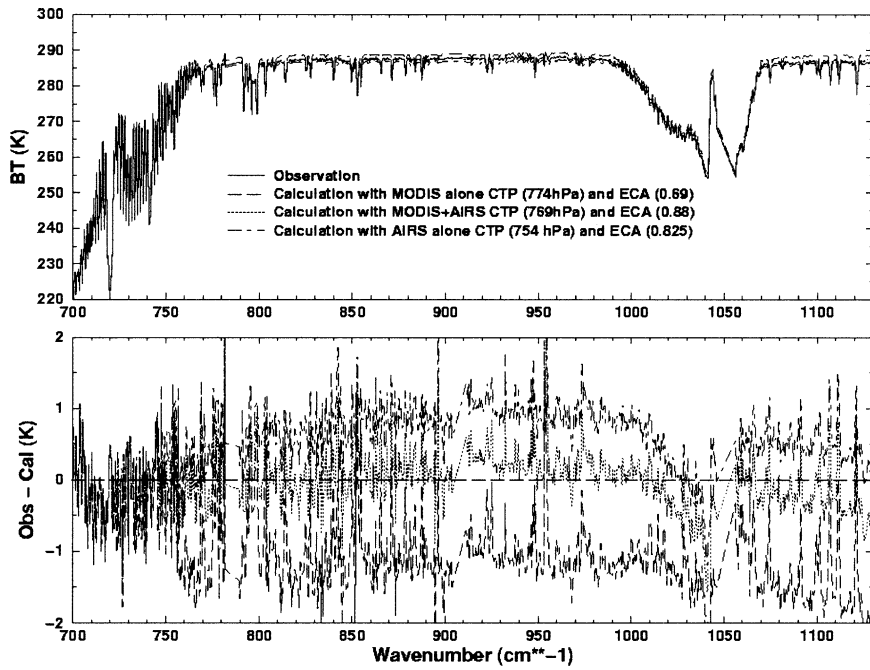


FIG. 6. As in Fig. 5, but for footprint F2 (see Fig. 4 for F2).

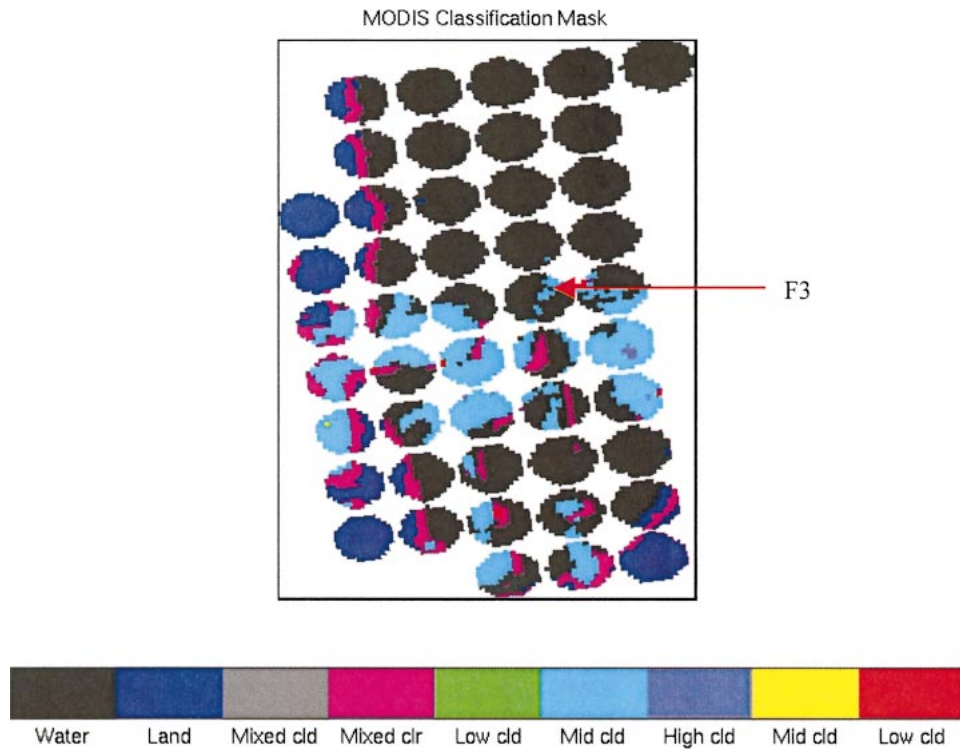


FIG. 7. The MODIS 1-km classification mask at 1-km spatial resolution for the Lake Michigan area A2 (see Fig. 1 for area A2) collocated to the AIRS footprints at 1920 UTC 6 Sep 2002.

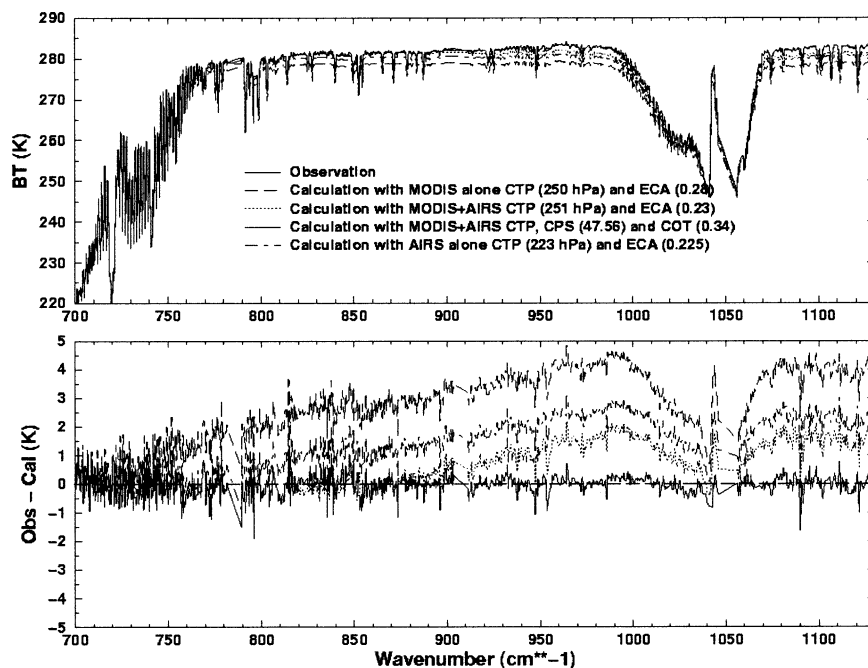


FIG. 8. As in Fig. 5, but for footprint F3 (see Fig. 7 for F3).

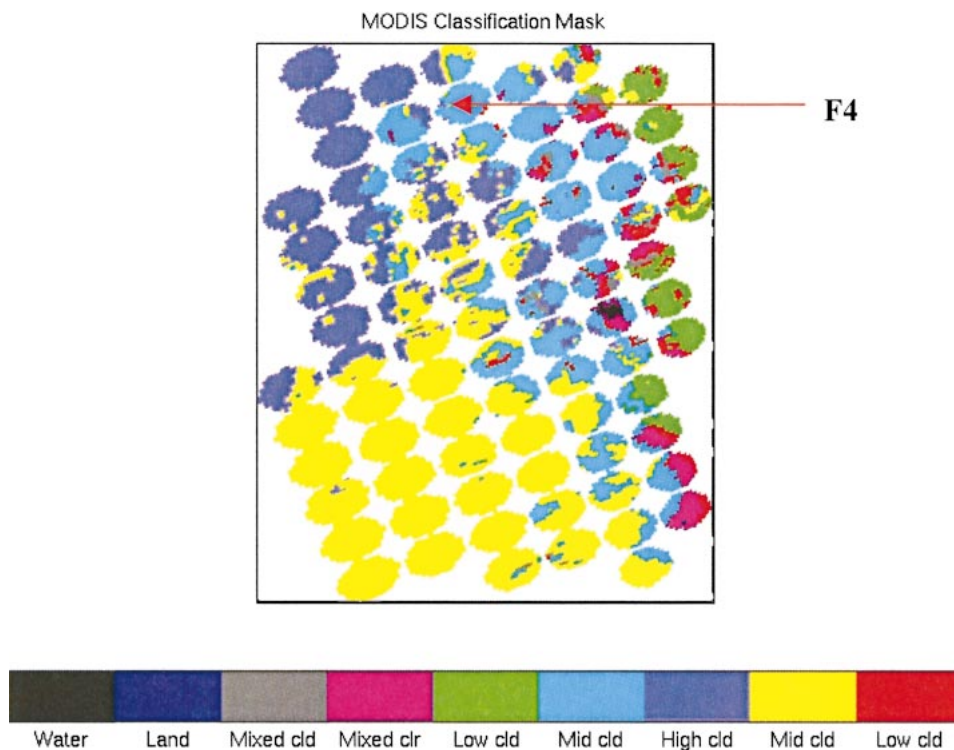


FIG. 9. The MODIS 1-km classification mask at 1-km spatial resolution for the study area A3 (see Fig. 1 for area A3) collocated to the AIRS footprints at 1920 UTC 6 Sep 2002.

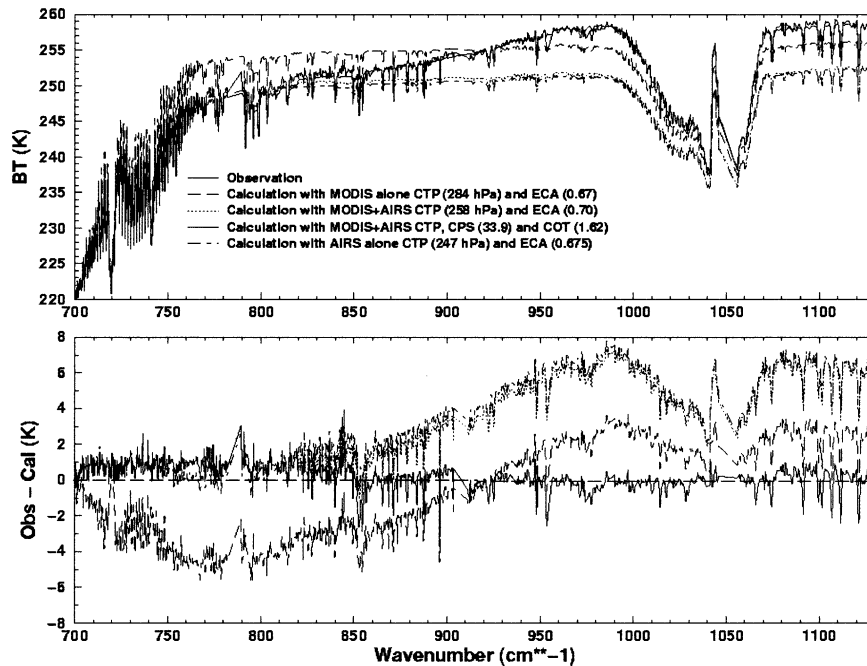


FIG. 10. As in Fig. 5, but for footprint F4 (see Fig. 9 for F4).

calculations with the MODIS-alone cloud products and the observation in the CO_2 region. However, the difference in the CO_2 region is almost removed by the calculation with the MODIS-AIRS-retrieved CTP and ECA; MODIS-AIRS adjusted the MODIS CTP by 26 hPa. MODIS-AIRS is slightly better than AIRS alone in this case. The slope of the BT in the spectral window region for F4 is significantly larger than that found in F3, suggesting a smaller CPS (Chung et al. 2000). With MODIS-AIRS-retrieved CPS and COT for this footprint, the calculation (solid line) fits the measurement (also solid line) slope very well, indicating that the cloud microphysical properties can be retrieved effectively from the AIRS radiance measurements.

MODIS provides useful cloud information, with high spatial resolution within an AIRS footprint, that includes the classification mask, cloud phase mask, and background information of CTP, ECA, CPS, and COT. The classification mask is derived from MODIS multispectral visible, NIR, and IR bands (Li et al. 2003), while the background information of CPS and COT is derived from MODIS visible and NIR bands (King et al 2003).

5. Discussion

Accuracy and efficiency of the MODIS-AIRS data collocation and the MODIS cloud phase/cloud classification determinations are very important when applying this technique of sounder subpixel cloud characterization in the MODIS-AIRS real-time data processing, and in future the ABI-HES data processing. Terrain corrections must be incorporated in future work to mitigate high-altitude collocation errors.

Classification accuracy is important for determining the multilayer clouds; sources of error have been addressed in Li et al. (2003). For the sounder subpixel cloud classification using imager radiance measurements, the significant questions are as follows: 1) Does the sounder footprint contain multilayer clouds? 2) If yes, how many layers exist in the footprint? Usually, it is not difficult to tell from the MODIS classification mask how many cloud types are contained in the AIRS footprint. Figure 11 shows the AIRS clear footprints (blue), single-layer cloud footprints (green), and multilayer cloud footprints (red) identified by the MODIS 1-km classification mask at 1920 UTC on 6 September 2002 (see Fig. 3 for the coverage). In this case 55% of the AIRS footprints appear to be clear, 22% indicate single-layer clouds, and approximately 23% are thought to be multilayer clouds.

The sources of error in the cloud phase determination are as follows: (a) cloud mask errors may produce errors in the cloud phase because the MODIS IR cloud phase algorithm is based on the MODIS cloud mask; (b) the MODIS IR cloud phase algorithm might misidentify water cloud phase as ice cloud phase at very cold BTs; and (c) there is a limitation on the MODIS IR phase algorithm for MODIS pixels that contain edges of clouds.

The algorithms and procedures must be made more efficient for routine or operational use. The current collocation procedure for an AIRS granule (usually the geographical coverage of one AIRS granule is equivalent to that of 2-3 MODIS granules) takes ~2-3 min on a Silicon Graphics, Inc. (SGI), Origin 2000 com-

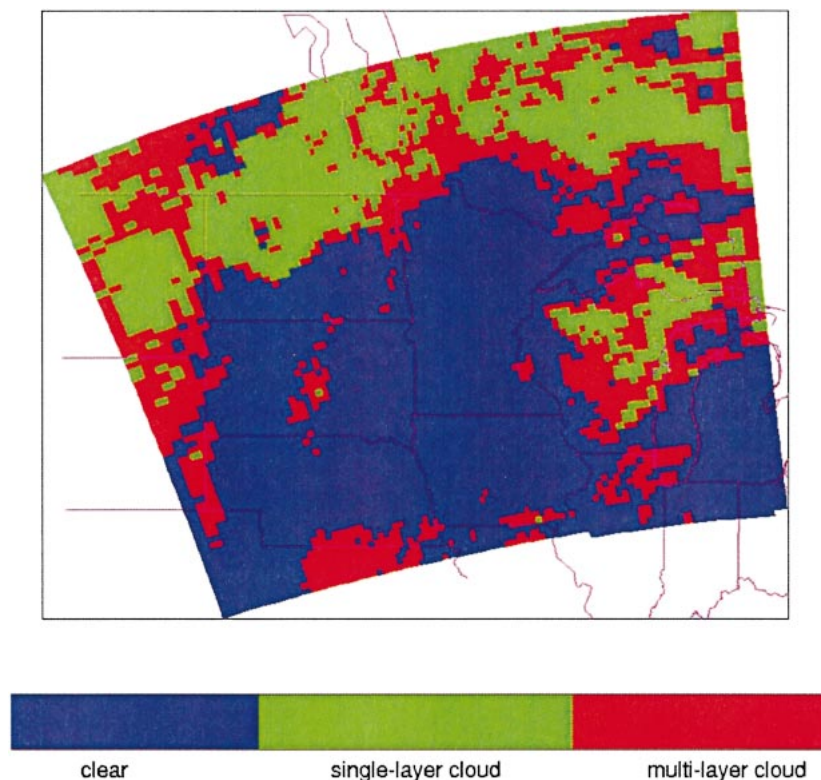


FIG. 11. The AIRS clear footprints (blue), single-layer cloud footprints (green), and multi-layer cloud footprints (red) identified by the MODIS 1-km classification mask at 1920 UTC 6 Sep 2002 (see Fig. 3 for the coverage).

puter or a Sun Microsystems, Inc., UNIX workstation. The classification procedure also takes several minutes.

6. Conclusions and future work

The following conclusions can be drawn from this study:

- 1) The MODIS cloud phase mask, with 1-km spatial resolution collocated to AIRS footprints, will help the cloud property retrieval from AIRS cloudy radiance measurements in some cases.
- 2) The MODIS classification mask with 1-km spatial resolution collocated to AIRS footprints can help to determine how many layers of clouds there are within each AIRS footprint. This is very important for initiating single-versus-multilayer cloud parameter retrievals with the AIRS cloudy radiance measurements within the single AIRS footprint. The MODIS classification mask collocated to AIRS footprints can also help to validate the retrievals of cloud parameters, such as ECA and COT.
- 3) Use of both MODIS and AIRS data enables better retrieval of cloud properties (CTP, ECA, CPS, and COT).

Future work includes more efficient MODIS classification procedures, and more efficient and more ac-

curate MODIS–AIRS collocation procedures, using the sounder subpixel cloud characterization for better retrieval of atmospheric and cloud parameters. In addition, classification based on AIRS channel radiance measurements will be studied; the AIRS classification result will be compared with the MODIS classification mask to demonstrate the similarities and differences between the two classification masks from high-spectral-resolution sounder radiance measurements and high-spatial-resolution imager radiance measurements, respectively. The calculations with cloud parameter retrievals from MODIS–AIRS synergism fit the AIRS-observed spectra better than with that from either MODIS cloud parameter retrievals or AIRS cloud parameter retrievals alone, demonstrating that the combination of MODIS and AIRS data provides cloud parameter retrievals with better accuracy. However, more validation needs to be done to quantify the improvements from MODIS–AIRS synergism. Ideally, lidar data should be used for validation; this will be the focus of future work. The operational products from MODIS and AIRS science teams, as well as validated measurements from other satellites such as GOES, will also be used for further comparison.

Acknowledgments. The authors thank Mr. Fred Nagle for creating the MODIS–AIRS collocation software. This work was partly funded by NOAA contracts re-

lating to the NOAA ABI-HES study NA07EC0676 and the NASA MODIS Science Team NAS5-31367. The views, opinions, and findings contained in this report are those of the authors and should not be construed as an official National Oceanic and Atmospheric Administration or U.S. Government position, policy, or decision.

REFERENCES

- Ackerman, S. A., K. I. Strabala, W. P. Menzel, R. A. Frey, C. C. Moeller, and L. E. Gumley, 1998: Determining clear sky from clouds with MODIS. *J. Geophys. Res.*, **103**, 32 141–32 157.
- Aumann, H. H., and Coauthors, 2003: AIRS/AMSU/HSB on the *Aqua* mission: Design, science objectives, data products, and processing systems. *IEEE Trans. Geosci. Remote Sens.*, **41**, 253–264.
- Baum, B. A., D. P. Kratz, P. Yang, S. C. Ou, Y. Hu, P. F. Soulen, and S. C. Tsay, 2000: Remote sensing of cloud properties using MODIS airborne simulator imagery during SUCCESS, 1, Data and models. *J. Geophys. Res.*, **105**, 11 767–11 780.
- Chung, S., S. A. Ackerman, P. F. van Delst, and W. P. Menzel, 2000: Model calculations and interferometer measurements of ice-cloud characteristics. *J. Appl. Meteor.*, **39**, 634–644.
- Eyre, J. R., 1989: Inversion of cloudy satellite sounding radiances by nonlinear optimal estimation. I: Theory and simulation. *Quart. J. Roy. Meteor. Soc.*, **115**, 1001–1026.
- Frey, R. A., S. A. Ackerman, and B. J. Soden, 1996: Climate parameters from satellite spectral measurements. Part I: Collocated AVHRR and HIRS/2 observations of spectral greenhouse parameter. *J. Climate*, **9**, 327–344.
- , B. A. Baum, W. P. Menzel, S. A. Ackerman, C. C. Moeller, and J. D. Spinhirne, 1999: A comparison of cloud top heights computed from airborne lidar and MAS radiance data using CO₂ slicing. *J. Geophys. Res.*, **104**, 24 547–24 555.
- Haertel, V., and D. A. Landgrebe, 1999: On the classification of classes with nearly equal spectral response in remote sensing hyperspectral image data. *IEEE Trans. Geosci. Remote Sens.*, **37**, 2374–2385.
- Hannon, S. E., L. L. Strow, and W. W. McMillan, 1996: Atmospheric infrared fast transmittance models: A comparison of two approaches. *Optical Spectroscopic Techniques and Instrumentation for Atmospheric and Space Research II*, P. B. Hays and J. Wang, Eds., International Society for Optical Engineering (SPIE Proceedings Vol. 2830), 94–105.
- King, M. D., and Coauthors, 2003: Cloud and aerosol properties, precipitable water, and profiles of temperature and water vapor from MODIS. *IEEE Trans. Geosci. Remote Sens.*, **41**, 442–458.
- Li, J., W. P. Menzel, Z. Yang, R. A. Frey, and S. A. Ackerman, 2003: High-spatial-resolution surface and cloud-type classification from MODIS multispectral band measurements. *J. Appl. Meteor.*, **42**, 204–226.
- , —, W. Zhang, F. Sun, T. J. Schmit, J. Gurka, F. Sun, and E. Weisz, 2004: Synergistic use of MODIS and AIRS in a variational retrieval of cloud parameters. *J. Appl. Meteor.*, in press.
- Menzel, W. P., and J. F. W. Purdom, 1994: Introducing GOES-I: The first of a new generation of geostationary operational environmental satellites. *Bull. Amer. Meteor. Soc.*, **75**, 757–781.
- , D. P. Wylie, and K. I. Strabala, 1992: Seasonal and diurnal changes in cirrus clouds as seen in four years of observations with VAS. *J. Appl. Meteor.*, **31**, 370–385.
- Nagle, F. W., 1998: The association of disparate satellite observations. *Proc. Second Symp. on Integrated Observing Systems*, Phoenix, AZ, Amer. Meteor. Soc., 49–52.
- Platnick, S., M. D. King, S. A. Ackerman, W. P. Menzel, B. A. Baum, J. C. Riedi, and R. A. Frey, 2003: The MODIS cloud products: Algorithms and examples from *Terra*. *IEEE Trans. Geosci. Remote Sens.*, **41**, 459–473.
- Rodgers, C. D., 1976: Retrieval of atmospheric temperature and composition from remote measurements of thermal radiation. *Rev. Geophys. Space Phys.*, **14**, 609–624.
- Schmit, T. J., J. Li, and W. P. Menzel, 2002: Advanced Baseline Imager (ABI) for future Geostationary Operational Environmental Satellites (GOES-R and beyond). *Applications with Weather Satellites*, W. P. Menzel et al., Eds., International Society for Optical Engineering (SPIE Proceedings Vol. 4895), 111–122.
- , W. F. Feltz, W. P. Menzel, J. Jung, A. P. Noel, J. N. Heil, J. P. Nelson III, and G. S. Wade, 2002: Validation and use of GOES sounder moisture information. *Wea. Forecasting*, **17**, 139–154.
- Smith, W. L., H. M. Woolf, C. M. Hayden, D. C. Wark, and L. M. McMillin, 1979: TIROS-N operational vertical sounder. *Bull. Amer. Meteor. Soc.*, **60**, 1177–1187.
- Strabala, K. I., S. A. Ackerman, and W. P. Menzel, 1994: Cloud properties inferred from 8–12- μm data. *J. Appl. Meteor.*, **33**, 212–229.
- Strow, L. L., S. E. Hannon, S. DeSouza-Machado, H. Motteler, and D. Tobin, 2003: An overview of the AIRS radiative transfer model. *IEEE Trans. Geosci. Remote Sens.*, **41**, 303–313.
- Susskind, J., D. Reuter, and M. T. Chahine, 1987: Cloud fields retrieved from analysis of HIRS2/MSU sounding data. *J. Geophys. Res.*, **92**, 4035–4050.
- , C. D. Barnet, and J. Blaisdell, 2003: Retrieval of atmospheric and surface parameters from AIRS/AMSU/HSB data in the presence of clouds. *IEEE Trans. Geosci. Remote Sens.*, **41**, 390–409.
- Yang, P., B. C. Gao, B. A. Baum, Y. X. Hu, W. J. Wiscombe, S. C. Tsay, D. M. Winker, and S. L. Nasiri, 2001: Radiative properties of cirrus clouds in the infrared (8–13 μm) spectral region. *J. Quant. Spectrosc. Radiat. Transfer*, **70**, 473–504.
- Zhang, H., and W. P. Menzel, 2002: Improvement in thin cirrus retrievals using an emissivity-adjusted CO₂ slicing algorithm. *J. Geophys. Res.*, **107**, 4327–4339.